Multi-Omic integration after carbon monoxide toxicity in a child reveals gene transcripts related to Parkinson and Multiple Sclerosis

Mara Leimanis (mara.leimanis@spectrumhealth.org)
Helen DeVos Children's Hospital https://orcid.org/0000-0003-0595-4578
Jeremy W. Prokop
Michigan State University
Derek Nedveck
Spectrum Health
Christina Darin
Michigan State University
Todd A. Lydic
Michigan State University
Caleb Bupp
Spectrum Health
Steven DeRoos
Helen DeVos Children's Hospital
Surender Rajasekaran
Helen DeVos Children's Hospital

Research article

Keywords: Gene, Transcriptome, Metabolites, Neurological injury, Toxin, Multiple Sclerosis

Posted Date: March 18th, 2020

DOI: https://doi.org/10.21203/rs.3.rs-17629/v1

Abstract

Background

This report highlights the unique transcriptomic and lipidomic changes noted in a 4-year-old African American female patient exposed to a house fire. She required admission to the pediatric Intensive care unit due to organ failure that resulted from CO and cyanide toxicity. Patient was neurologically intact initially but later developed neurological symptoms consistent with Parkinsonism, a transient state resembling Parkinson's Disease.

Results

An integrative omics-based approach was used to examine both gene expression and the lipidome of the patient which was then compared to 4 control patients. Total blood RNA from a PaxGene®collection system was correlated to plasma-based metabolomics measured over three time points and correlated with the clinical condition of the patient. We see significant elevation of the Parkinson's associated gene (SELENOT) on day one. This gene plays a crucial role in the protection of dopaminergic neurons against oxidative stress in Parkinson's disease. The Multiple Sclerosis linked gene DDX39B which mediates ATP hydrolysis during pre-mRNA splicing was increased on day 8. We noted increased UGCG gene expression which correlated with increased ceramide lipids on lipidome analysis. The elevated ratio of hexosylceramide to its ceramide precursor is indicative of an elevated UGCG mediated ceramide glucosyltransferase activity. This correlation of clinical symptoms with both increased gene activity and lipid dyshomeostasis is unique, highlighting the potential of personalized omics.

Conclusions

In clinical practice, the ability to predict and quantify neurological injury using gene expression has the potential to make meaningful changes to management. This report shows the potential for real time transcriptomics and metabolomics to modify not only initial therapy, but the eventual physical rehabilitation of patients exposed to neurotoxins.

Background

Neurotoxins such as carbon monoxide (CO) mediate their effect in a pleotropic fashion where the neurologic deficits do not necessarily correlate with blood CO levels but from the effects of CO on cellular mitochondrial respiration, inflammation, and free radical generation, especially in the brain and heart. Long-term neurocognitive deficits occur in 15–40% of patients. Thus, the effects of toxins lend themselves well to multi-omic characterization. There are essentially no DNA-based syndromes or well-established conditions that could be investigated in relationship to CO, highlighting the utility of using other omics. The patient was exposed to CO and cyanide by a house fire occurring while she was asleep. The patient was initially treated with 100% normobaricoxygen, and then intubated and mechanically ventilated, the most common treatment for CO toxicity [24]. Neurological injury is well documented after

CO toxicity, with reports of patients that range from transient neurologic deficits to chronic debilitating diseases such as Parkinson's disease and multiple sclerosis after exposure to CO. [17, 18, 27]. The patient presented here suffered from neurological outcomes, where we were able to, for the first time ever, uncover potential mechanisms for neurological outcomes using a multi-time point, multi-omics strategy.

Results

We describe novel transcriptomic and lipidomic characterization of biological pathways in a 4-year-old African American female patient exposed to CO and cyanide from a house fire with blood collected at time points before, during, and after treatment. Patient presented to a local emergency department with a CO level of 32.5%, and was immediately intubated and administered 100% oxygen and hydroxycobalamin for the cyanide poisoning. She was transferred to the pediatric intensive care unit (PICU) and received one administration of hyperbaric therapy at 2.5 atmospheres for 60 minutes resulting in the immediate drop of CO levels to 0.02%, and to 0.0% by day 3. The initial cyanide level of 684 micrograms/dL (normal < 200 micrograms/dL) dropped to 3.7 micrograms/dL by day 3.

Bronchoscopy confirmed soot in vocal cords and airway inflammation. Patient appeared neurologically intact but was intubated for airway protection soon after due to the inhalational injury. Her PICU course was initially characterized by cardiopulmonary dysfunction and later by neuromuscular dysfunction.

During the second week of PICU admission, neurological symptoms predominated, with neuromotor deficits including impulsiveness, right-sided weakness, and ataxia with bradykinesia and tremors described as Parkinsonian. Magnetic resonance imaging (MRI) and electroencephalogram done at this time were normal. The patient received treatment in the PICU for nine days and was discharged on day 13 with plans for outpatient rehabilitation at the family's request.

Patient had a total of 261 (209 up / 52 down), 74 (33 / 41), and 44 (16 / 38) differentially expressed genes (DEGs) relative to controls at day 0, day 3, and day 8 respectively, suggesting many genes normalized by day 3. From annotation of transcripts uniquely elevated in the patient (Supplemental Table), we see significant elevation of the CHD9, CD177, S100A8, Parkinson's associated SELENOT specific to day 0; elevation of DEFA1, DEFA3, PDAP1, Multiple Sclerosis linked DDX39B at day 8; elevation of Beta2-microglobulin (B2M), CANX, TSEN34, SERPINA1, B3GALT4, UBE2F, ACP5, and NAA25 at all days in the patient relative to the controls. Additional DEGs at day 0 involved immune system responses and glycolytic processes (GO:0002376, 0006955, 0006952, 0045087, 0006096), Hypoxia Inducible Factor-1 (HIF-1) signaling pathway (KEGG:04066) and hematopoietic cell lineage (KEGG:04640). The patient had some enrichment in immune system function at day 8, though clustered similarly with controls (Fig. 1A). Genes involved in neutrophil degranulation and activation of reactive oxygen species were found to differ temporally (GYG1, CLEC5A, GPR84, CYSTM1, MCEMP1, SERPINB1, RETN, MMP8, CD177) as well as UGCG (log2 fold change of 2.1 from baseline to day 3–8), also known as ceramide glucosyltransferase enzyme involved in lipid synthesis (Fig. 1B).

Lipidomics of patient at day 0 compared to 8 (Fig. 1C) revealed increased ratio of hexosylceramide/ceramide, mono-unsaturated/saturated phosphatidylcholine, and levels of total monoacylglycerides and diacyglycerides (Fig. 1D). Triglycerides at day 0 (Fig. 1E) and sphingomyelins at day 8 (Fig. 1F) were elevated. She returned for follow up three years later where after a comprehensive history and physical we found she may have more subtle learning issues related to her injury. We found no neurologic deficits on examination.

Discussion And Conclusions

In this report we describe the use of multi-omics in a 4-year-old with neurological injury from CO toxicity to characterize her clinical course. Early on, she had signs of a hyper-inflammatory response such as respiratory failure, hemodynamic instability and later developed neurologic deficits. These clinical findings correlated with the early increase in HIF-1 pathway expression changes along with genes governing cytokine release and neutrophil activation (Fig. 1G), as has been previously shown [25].

RNA expression revealed transcripts from a complexity of genomic responses and lipidome changes not previously documented in CO toxicity. We showed that not only were there transcriptomic changes like the upregulation of UGCG gene but its correlation with actual changes in metabolite ceramide lipids. The elevated ratio of hexosylceramide to its ceramide precursor (Fig. 1D) that we were able to reveal is consistent with elevated ceramide glucosyltransferase activity. This gene has been suggested as an overlap between immune system neutrophil lipid regulation and neural glial regulation [14, 21], and linked with a multidrug resistance protein [29], a gene known and described to have a role in Parkinson's disease [1]. Elevated 2-hydroxy ceramide at day 8 could be related to the neurological injury noted in the patient as 2-hydroxy ceramide is known to be critical for myelin sheath stability of oligodendrocytes [30].

By using transcript abundances over that of the compiled gene levels we were able to highlight multiple neurological gene transcripts. Amongst the top candidates is that of B2M, which was altered relative to controls. B2M gene is expressed in dopaminergic neurons [19] and blood and is associated with aging-based neurological function [26]. Other transcripts seen elevated (Day 0–8), include the endoplasmic reticulum associated chaperone CANX, the splicing factor TSEN34 (associated with pontocerebellar hypoplasia) [22], and the Parkinson's dementia marker SERPINA1 [11]. On day 8, there was an elevation of the transcript ENST00000455645 that codes for a variant of the DDX39B gene known to contribute to multiple sclerosis through regulating splicing of IL7R [9], suggesting an immune dysregulation of nerve cell function that overlaps with the patient's phenotype.

Omics have the potential to change clinical therapy, highlighted classically by oncological diseases. In this study, using N = 1 data, we were able to correlate the transcriptome and lipidomic signaling tying them to actual clinical events. One could hypothetically use such data to manage patients in the future such as the deciding the number of hyperbaric administrations or initiate therapy for downstream injury earlier. There have been previous proposals to target the downstream effects of CO poisoning such as the inflammation or oxidative stress [24]. Currently, therapy is determined purely by the CO level and is

otherwise entirely reactive. Proposals such as these have faltered for a lack of measurable biomarkers that can drive therapy. The distribution of transcripts could drive discovery of biomarkers and be used to design more focused clinical trials that adhere more closely to precision medicine principles.

A traditional genomics approach to disease would interrogate the genome for mutations, variants, or perhaps findings suggested by genome-wide association studies. The genes noted to have alterations in this presented transcriptome, of which would be difficult to identify abnormalities to classify, given there are no well-established genomic conditions associated with them. At best, it might be possible to quantify some risk factor from those genes, but not enough to provide disease etiology or guide management. Utilizing non-genomic modalities such as transcriptomics and lipidomics opens the window into physiologic function in a way that standard genomics cannot. They also can provide results in a more time effective manner, which is crucial to the ability to impact care. Lastly, this approach serves notice of the vast potential for understanding acute illness not related to a baseline disease such at CO toxicity in ways that have simply not been possible to date.

The goal of therapy in CO toxicity is to preserve life and minimize neurological injury. This requires an understanding of the cytopathic mechanisms related to CO poisoning. It is well known that patients can suffer from long-term neurocognitive sequelae related to brain injury [27]. In this child, hypoxic signaling related to the toxidrome predominated early and despite hyperbaric therapy, the patient developed neurological manifestations. The associated lipidomic signatures such as SM(d18:1/18:2), previously linked with Alzheimer's disease [12], and the other Parkinson related genes that were elevated reveal tissue injury more precisely than conventional imaging such as MRI, which was negative in our patient. We also highlight lipids as being more suitable than proteins for biomarker discovery because they are more suited for the frenetic nature of the ICU as they are easily preservable [2].

This case study highlights the untapped resource of transcriptomics and lipidomics for studying toxic exposures and espousing its eventual utility as precision medicine tools. This is the first report to integrate these tools to uncover the expression of genes and mediators related to neuro-debilitating diseases such as Parkinson's or multiple sclerosis in CO toxicity.

Methods

This patient makes up part of our IRB approved (2016-062-SH/HDVCH) precision medicine initiative to characterize patients admitted to our Pediatric ICU with multi-organ dysfunction syndrome. A prospective repeated measures design was adopted to assess the transcriptome profiles from patients of the pediatric intensive care unit at a high-volume tertiary care facility in Western Michigan. Specifically, patients who were acutely and critically ill, with at least two organs failing, were screened for eligibility and subsequently approached for consent as a consecutive series of patients. Blood samples were collected at up to 3 independent time points, at baseline (day 0), > 48 hours to < 72 hours (day 3), and > 7 days (day 8). These time points were collected to reflect the trajectory of critical illness with measurements in the acute, stabilization, and recovery phases of illness.

Sample

Patients were enrolled according to the first consecutive series of patients from September 2016 through May 2017. Samples were serially collected at the time of consent (baseline), day 3, and day 8. The sedation patients who served as healthy controls had only one sample drawn at one time point. Inclusion criteria were the following: patients < 18 years of age, patients on vasopressors and requiring additional oxygen supplementation, sedation-healthy control patients presenting for routine sedation in an outpatient clinic without an inflammatory disease, and patients with a central line. Following sample collection, PaxGene® tubes were stored according to the manufacturer's recommendations at room temperature for at least 2 hours, overnight at -20 °C, and at -80 °C for long-term storage. Blood samples were drawn in EDTA-filled anticoagulant and spun twice on site in a refrigerated centrifuge (15 min at 400 xg; 1500 rpm, 10 min at 10,000 xg; 10,000 rpm), plasma was frozen overnight at -20 °C and at -80 °C for long-term storage.

RNA extraction from PAXgene blood tubes

PAXgene whole Blood RNA tubes were removed from − 80 °C, allowed to thaw at room temperature for 2 hours, and processed according to Qiagen's QIAsymphony PAXgene Blood RNA Kit protocol. The cell lysate underwent RNA extraction, including a DNA digestion, on the QIAsymphony using the PAX_RNA_V5 protocol. RNA was eluted in 80 µL Buffer BR5 and stored at -80 °C until further processing.

Construction and Sequencing of Directional total RNA-seq Libraries

A total of 2 ug of RNA was cleaned using ZR-96 Clean and Concentrator column (Zymo Research). Globin ribosomal RNAs were depleted using the Globin Zero-Gold rRNA kit (Illumina) followed by RNAseq library preparation using the KAPA RNA HyperPrep Kit (v1.16) (Kapa Biosystems, Wilmington, MA USA). RNA was sheared to 300–400 bp. Prior to PCR amplification, cDNA fragments were ligated to Bio Scientific NEXTflex Adapters (Bio Scientific, Austin, TX, USA). Quality and quantity were assessed using Agilent DNA High Sensitivity chip (Agilent Technologies, Inc.), QuantiFluor® dsDNA System (Promega Corp., Madison, WI, USA), and Kapa Illumina Library Quantification qPCR assays (Kapa Biosystems). Individually indexed libraries were pooled and 75 bp, paired-end sequencing was performed on an Illumina NextSeq 500 sequencer using a 150 bp sequencing kit (v2) (Illumina Inc., San Diego, CA, USA), with all libraries run across 7 flowcells in paired-end approach. Base calling was done by Illumina NextSeq Control Software (NCS) v2.0. The output of NCS was demultiplexed and converted to FastQ format with Illumina Bcl2fastq v1.9.0.

Lipidomics

Lipidome profiles were determined from frozen plasma, subjected to lipid extraction with acetone, methanol, and acetonitrile [4], and analyzed by nano-electrospray direct infusion high resolution/accurate mass spectrometry and tandem mass spectrometry utilizing an LTQ-Orbitrap Velos mass spectrometer (Thermo Scientific, Waltham, MA) with the FT analyzer operating at 100,000 resolving power, over two

minutes. An Advion Nanomate Triversa (Advion Biosciences, Ithaca, NY) served as the nano-electrospray source and high-throughput autosampler. To verify lipid identities, Higher-Energy Collisional Dissociation was utilized (at 100,000 resolving power). Global lipidome analysis provided untargeted analysis with detection limits of 0.01 nM to 10 nM. Each sample was run twice (positive ion and negative ion analysis) and data was combined. Di-myristoyl phosphatidylcholine served as an internal standard. Peak finding and quantification for global lipidomics and targeted lipid mediators was performed with Lipid Mass Spectrum Analysis (LIMSA) version 1.0 software [10] and MAVEN software [5], respectively.

Transcriptomic analysis

Paired-end reads from fastq files were run in Salmon [18] using the Ensembl 96 transcript library. DEGs in DESeq2 [28] compared each patient time point to four healthy, sedated pediatric controls. DEGs, adjusted p-value < 0.10, were used in enrichment analysis for Gene Ontology and KEGG pathways. Visualized differences between time points used > 5 TPM (Transcripts Per Million reads sequenced) and log2 fold changes relative to controls ≥ 2 or ≤ -2. To calculate day 0, day 8, and all day elevated transcripts we used the following enrichment calculations: Day0_enrichment= (Day0_TPM) x ((Day0_TPM - control_TPM)/control_StDev) x log2(Day0_TPM/Day8_TPM); Day8_enrichment= (Day8_TPM) x ((Day8_TPM - control_TPM)/control_StDev) x log2(Day8_TPM/Day0_TPM).

List Of Abbreviations

Carbon monoxide (CO); Pediatric intensive care unit (PICU); Magnetic resonance imaging (MRI); Differential expression genes (DEGs); Beta2-microglobulin (B2M); Hypoxia Inducible Factor-1 (HIF-1); NextSeq Control Software (NCS); Mass Spectrometry (MS); Lipid Mass Spectrum Analysis (LIMSA); Transcripts per million (TPM)

Declarations

Ethics approval and consent to participate

Our study was approved by Spectrum Health IRB (SH/HDVCH-2016-062), and the family consented before samples were drawn.

Consent for publication

Approval was obtained from the family for publications.

Availability of data and materials

The datasets generated and/or analyzed during the current study are not publicly available due to their upcoming release in a subsequent manuscript (currently submitted), but are available from the corresponding author upon reasonable request.

Competing interests

The authors declare that they have no competing interests.

Funding

Funding for this project was provided by Spectrum Health Office of Research (SHOR) funding initiative for precision medicine (SR, ML) and NIH Office of the Director and NIEHS grant K01ES025435 (JWP).

Authors' contributions

RS, ML conceived of the study design, consented the patients, collected study samples, coordinated sample processing, obtained all necessary IRB approvals, and funding. TL processed and identified the lipidomic samples. JP, DN analyzed the data. RS, ML, TL, CB, JP, DN, CD, SD wrote the manuscript and contributed to the editing process. All authors read and approved the final manuscript.

Acknowledgments

The authors thank Brittany Essenmacher, who helped in editing the final manuscript and submission.

References

1. Ahmed SSSJ, Husain RSA, Kumar S, Ramakrishnan V. Association between MDR1 gene polymorphisms and Parkinson's disease in Asian and Caucasian populations: a meta-analysis. J Neurol Sci. 2016;doi: 10.1016/j.jns.2016.07.041.
2. Anderson NL, Anderson NG. The human plasma proteome: history, character, and diagnostic prospects. Mol Cell Proteomics MCP. 2002;doi: 10.1074/mcp.r200007-mcp200.
3. Armitage EG, Southam AD. Monitoring cancer prognosis, diagnosis and treatment efficacy using metabolomics and lipidomics. Metabolomics. 2016;doi: 10.1007/s11306-016-1093-7.
4. Cai X, Li R. Concurrent profiling of polar metabolites and lipids in human plasma using HILIC-FTMS. Scientific reports. 2016;doi:10.1038/srep36490.
5. Clasquin MF, Melamud E, Rabinowitz JD. LC-MS data processing with MAVEN: a metabolomic analysis and visualization engine. Curr Protoc Bioinformatics. 2012;doi:10.1002/0471250953.bi1411s37.
6. Fall N, Barnes M, Thornton S, Luyrink L, Olson J, Ilowite NT, et al. Gene expression profiling of peripheral blood from patients with untreated new-onset systemic juvenile idiopathic arthritis reveals molecular heterogeneity that may predict macrophage activation syndrome. Arthritis Rheum. 2007;doi:10.1002/art.22981.
7. Fhaner CJ, Liu S, Ji H, Simpson RJ, Reid GE. Comprehensive lipidome profiling of isogenic primary and metastatic colon adenocarcinoma cell lines. Anal Chem. 2012;doi:10.1021/ac302154g.
8. Fhaner CJ, Liu S, Zhou X, Reid GE. Functional group selective derivatization and gas-phase fragmentation reactions of plasmalogen glycerophospholipids. Mass Spectrom (Tokyo). 2013;doi:10.5702/massspectrometry.S0015.

9. Galarza-Muñoz G, Briggs FBS, Evsyukova I, Schott-Lerner G, Kennedy EM, Nyanhete T, et al. Human Epistatic Interaction Controls IL7R Splicing and Increases Multiple Sclerosis Risk. 2017;doi: 10.1016/j.cell.2017.03.007.
10. Haimi P, Uphoff A, Hermansson M, Somerharju P. Software tools for analysis of mass spectrometric lipidome data. Anal Chem. 2006;doi:10.1021/ac061390w.
11. Halbgebauer S, Nagl M, Klafki H, Haußmann U, Steinacker P, Oeckl P, et al. Modified serpinA1 as risk marker for Parkinson's disease dementia: Analysis of baseline data. Sci Rep. 2016;doi: 10.1038/srep26145.
12. Han X, Rozen S, Boyle SH, Hellegers C, Cheng H, Burke JR, Conde JG. Metabolomics in early Alzheimer's disease: identification of altered plasma sphingolipidome using shotgun lipidomics. PLoS One. 2011;doi:10.1371/journal.pone.0021643.
13. Harris PA, Taylor R, Thiekle R, Payne J, Gonzalez N, et al. Research electronic capture (REDCap) - A metadata-driven methodology and workflow process for providing translational research informatics supports. Journal of Biomedical Information. 2009;42:377-381.
14. Ishibashi Y, Kohyama-Koganeya A, Hirabayashi Y. New insights on glucosylated lipids: metabolism and functions. Biochim Biophys Acta. 2013;doi: 10.1016/j.bbalip.2013.06.001.
15. Kortz L, Dorow J, Becker S, Thiery J, Ceglarek U. Fast liquid chromatography-quadrupole linear ion trap-mass spectrometry analysis of polyunsaturated fatty acids and eicosanoids in human plasma. J Chromatogr B Analyt Technol Biomed Life Sci. 2013;doi:10.1016/j.jchromb.2013.03.012.
16. Kossenkov AV, Qureshi R, Dawny NB, Wickramasinghe J, Liu Q, Majumdar RS, et al. A Gene Expression Classifier from Whole Blood Distinguishes Nenign from Malignant Lung Nodules Detected by Low-Dose CT. Cancer Res. 2019;doi: 10.1158/0008-5472.CAN-18-2032.
17. Lai CY, Chou MC, Kao CH. Increased rick of Parkinson disease in patients with carbon monoxide intoxication: a population-based cohort study. Medicine (Baltimore). 2015;doi: 10.1097/MD.0000000000000869.
18. Lavery AM, Waubant E, Casper TC, Roalstad S, Candee M, Rose J, et al. Urban air quality and associations with pediatric multiple sclerosis. Ann Clin Transl Neurol. 2018;doi: 10.1002/acn3.616.
19. Lindå H, Hammarberg H, Piehl F, Khademi M, Olsson T. Expression of MHC class I heavy chain and beta2-microglobulin in rat brainstem motoneurons and nigral dopaminergic neurons. J Neuroimmunol. 1999;101:76–86.
20. Lydic TA, Townsend S, Adda CG, Collins C, Mathivanan S, Reid GE. Rapid and comprehensive 'shotgun' lipidome profiling of colorectal cancer cell derived exosomes. Methods. 2015;doi:10.1016/j.ymeth.2015.04.014.
21. Mondal N, Stolfa G, Antonopoulos A, Zhu Y, Wang S-S, Buffone A, et al. Glycosphingolipids on Human Myeloid Cells Stabilize E-Selectin-Dependent Rolling in the Multistep Leukocyte Adhesion Cascade. Arterioscler Thromb Vasc Biol. 2016;doi: 10.1161/ATVBAHA.115.306748.
22. Namavar Y, Barth PG, Poll-The BT, Baas F. Classification, diagnosis and potential mechanisms in pontocerebellar hypoplasia. Orphanet J Rare Dis. 2011;doi: 10.1186/1750-1172-6-50.

23. Patro R, Duggal G, Love MI, Irizarry RA, Kingsford C. Salmon provides fast and bias-aware quantification of transcript expression. Nat Methods. 2017;doi:10.1038/nmeth.4197.
24. Rose JJ, Wang L, Xu Q, McTiernan CF, Shiva S, Tejero J, et al. Carbon Monoxide Poisoning: Pathogenesis, Management, and Future Directions of Therapy. Am J Respir Crit Care Med. 2017;doi: 10.1164/rccm.201606-1275CI.
25. Schnittger V, Rosendahl K, Lind F, Palmblad J. Effects of carbon monoxide poisoning on neutrophil responses in patients treated with hyperbaric oxygen. J Investig Med Off Publ Am Fed Clin Res. 2004;doi: 10.1136/jim-52-08-24.
26. Smith LK, He Y, Park J-S, Bieri G, Snethlage CE, Lin K, et al. β2-microglobulin is a systemic pro-aging factor that impairs cognitive function and neurogenesis. Nat Med. 2015;doi: 10.1038/nm.3898.
27. Sykes OT, Walker E. The neurotoxicology of carbon monoxide - Historical perspective and review. Cortex J Devoted Study Nerv Syst Behav. 2016;doi: 10.1016/j.cortex.2015.07.033.
28. Szklarczyk D, Morris JH, Cook H, Kuhn M, Wyder S, Simonovic M, et al. The STRING database in 2017: quality-controlled protein-protein association networks, made broadly accessible. Nucleic Acids Res. 2017;doi:10.1093/nar/gkw937.
29. Wegner M-S, Gruber L, Mattjus P, Geisslinger G, Grösch S. The UDP-glucose ceramide glycosyltransferase (UGCG) and the link to multidrug resistance protein 1 (MDR1). BMC Cancer. 2018;doi: 10.1186/s12885-018-4084-4.
30. Zöller I, Meixner M, Hartmann D, Büssow H, Meyer R, Gieselmann V, et al. Absence of 2-hydroxylated sphingolipids is compatible with normal neural development but causes late-onset axon and myelin sheath degeneration. J Neurosci Off J Soc Neurosci. 2008;doi: 10.1523/JNEUROSCI.0458-08.2008.

Figures

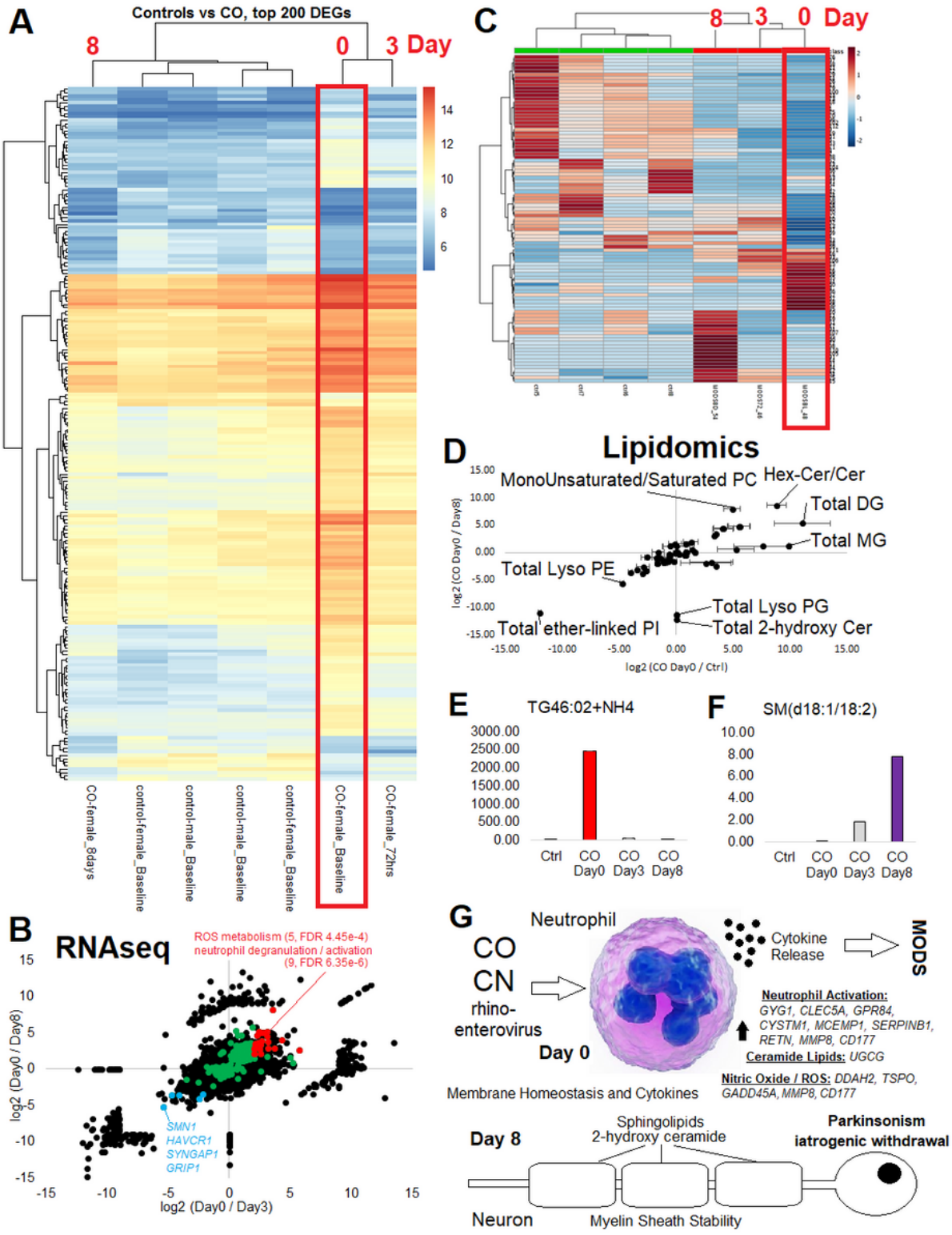

Figure 1

Omics of patient. A) Heatmap of differentially expressed genes (DEGs) in the patient (red box) relative to four controls. Blue values are lower and red values are higher. Dendrograms on the side show the clustering of genes and on the top the clustering of patient blood collections at day 0, day 3 and a second cluster of the patient at day 8 with the four controls. B) Gene expression changes in the patient from day 0 relative to day 3 (x-axis) and day 8 (y-axis) of treatment, shown as log2 fold changes. DEGs identified in

panel A are colored in green, and those in red and cyan are significant between day 0 and day3/8. C) Heatmap of lipidomics showing clustering of patient three-day measures relative to controls. D) Lipidomics of patient showing log2 fold change of patient at day 0 relative to day 8 (y-axis) and patient day 0 relative to the four controls (x-axis). Error bars represent the SEM of the patient relative to the four controls. E) Representative triglyceride (TG) that is elevated at day 0 only in the patient. F) Representative sphingomyelin (SM) that is elevated by day 8 in the patient. G) Pictorial of patient case and omics data.

Supplementary Files

This is a list of supplementary files associated with this preprint. Click to download.

- SupplementalTableS1Sept19th2019.xlsx